The Possible Hepatoprotection Promoted by Melatonin and Alpha-Tocopherol in Acrylamide-Induced Liver Injury in Male Albino Rats: A Histological and Immunohistochemical Study

Hend R. Mousa[1], Ahmed A. Morsi[3] and Lamiaa M. Shawky[2]

[1]Department of Anatomy, [2]Department of Histology and Cell Biology, Faculty of Medicine, Benha University, Benha, Egypt

[3]Department of Histology and Cell Biology, Faculty of Medicine, Fayoum University, Fayoum, Egypt

ABSTRACT

Introduction: Acrylamide (ACR) is commonly polluting the nearby environment as it is formed during high-temperature food cooking conditions. Several previous studies have confirmed its toxic potential on different body organs.

Aim of the Work: The current study aims to investigate the possible hepatoprotection elicited by vitamin E (vit E), alpha-tocopherol, melatonin (MT), and combined vit E/MT in a rat model of ACR-induced liver toxicity. The putative mechanisms involved in such protection were also examined using histological and immunohistochemical studies.

Material and Methods: Forty-nine male Wistar albino rats were divided into seven equal groups; control, vit E alone (100 mg/kg/d), MT alone (10 mg/kg/d), ACR-exposed (5 mg/kg/day), ACR/vit E-treated, ACR/MT-treated, and ACR/vit E/MT-treated groups. All treatments were given daily via oral gavage for 8 weeks. At the end of the study, blood samples were collected for measurement of the liver enzymes. Liver lobes were collected for preparation of the tissue homogenates to measure the hepatic concentrations of the oxidative/antioxidative markers. Also, liver samples were prepared for paraffin microtechniques and stained by Hematoxylin & Eosin (H & E) and Masson trichrome staining. Immunohistochemical assays for the detection of Bax, Bcl2, and iNOS immunoexpressions were performed.

Results: ACR-exposed rats showed marked disruption of the biochemical assays, in addition to the hepatocytes disorganization and vacuolar degenerative changes observed in the H & E findings. Moreover, fibrotic changes in the Masson-stained sections and disturbed immunoexpressed proteins were noticed. Either vit E and/or MT treatment improved the histological and biochemical parameters with normalization in the combined therapy group.

Conclusion: Vit E and or MT protected against ACR-mediated liver toxicity by reestablishing of the oxidant/antioxidant balance, downregulation of pro-apoptotic proteins, upregulation of anti-apoptotic proteins, and suppression of the inflammatory pathways. Both combined had a synergistic action.

INTRODUCTION

Acrylamide (ACR) is a common environmental pollutant characterized by being white, crystalline, water-soluble, and odorless. ACR doesn't exist in nature under normal conditions; however, it is formed during high-temperature cooking conditions (≥120 ℃) such as roasting, frying, and baking, through the Maillard reaction. A chemical change occurs in protein and carbohydrate foodstuffs exposed to high-temperature characterized by brown crust formation on food surfaces due to the formation of harmful byproducts such as acrylamide and 5-hydroxymethylfurfural. So, it is extensively found in several food products including oven-baked, deep-fried foods, biscuits, chips, bread, and coffee[1]. Moreover, it is used in industrial processes e.g. gel electrophoresis, papers and dyes manufacturing, wastewater treatment and tertiary oil recovery[2].

Owing to its water solubility and low molecular weight, ACR has the capability to cross the biological tissue membranes such as placental and blood-milk barriers, hence its neurotoxic, reproductive, genotoxic, carcinogenic, and hepatotoxic effects[3].

Alpha-tocopherol, vitamin E (vit E) is a plant-derived lipid-soluble antioxidant compound naturally found in biological systems. It provides cellular protection against cell membrane peroxidation caused by reactive oxygen species (ROS) overproduction. Being a "chain breaker", alpha-tocopherol breaks the lipid peroxidation chain reactions by giving its phenolic hydrogen to a lipid peroxyl

radical (LOO) leading to the formation of non-reactive lipid hydroperoxide (LOOH) and α-tocopheroxyl radical[4]. Recent studies[5,6,7] demonstrated a cytoprotective effect for vit E in various animal models of acute and chronic liver toxicity indicating that vit E may have a potential efficacy in ameliorating ACR-mediated liver injury.

Melatonin (MT) is a powerful natural antioxidant hormone released by the pineal gland, has a vital role in sleep and circadian rhythms regulation, immune system function, and elimination of oxygen free radicals[8]. Melatonin could enhance the upregulation of antioxidants and antioxidant enzymes such as superoxide dismutase, and glutathione reductase, so neutralizes the effects of both nitrogen and oxygen-reactive molecules. Furthermore, anti-inflammatory, anti-apoptotic, and anti-cancer activities have been reported for MT[9].

Based on these literature data, the exogenous administration of MT might be a beneficial strategy to manage the liver damage induced by ACR. However, the therapeutic efficacy of MT and its related molecular mechanism on liver injury caused by chronic ACR exposure need to be further studied. Given these considerations, it was agreed that further research on the therapeutic potential of vitamin E versus melatonin against ACR hepatotoxicity would be interesting. Therefore, the present study aimed to elucidate whether Vitamin E and melatonin can ameliorate the hepatic damage induced by ACR using histopathological and biochemical approaches.

MATERIALS AND METHODS

Drugs and chemicals

Acrylamide (ACR) powder (product number: A3553, ≥ 99% purity), alpha-tocopherol liquid (product number: T3251, ≥ 96% purity), and melatonin powder (product number: M5250, ≥ 98% purity) were purchased from Sigma Aldrich (St. Louis, Missouri, USA).

Preparation of acrylamide, alpha-tocopherol, and melatonin

Acrylamide powder was dissolved in distilled water and was given via oral gavage to the animals, 5 mg/kg/day for 8 weeks[10]. Alpha-tocopherol (1 mL) was diluted in olive oil (19 mL) to reach a final concentration of 50 mg/mL and was given in a dose of 100 mg/kg/d[6]. Melatonin (25 g) was freshly dissolved in 100 % ethanol (5 mL) and diluted in normal saline (4.995 L) to reach a final concentration of 5 mg/mL and was given in a dose of 10 mg/kg/d. The volume of saline (4.995 L) was used to make the final ethanol concentration, in the prepared solution, was not exceeding 0.1%[11].

Animals and experimental groups

Forty-nine adult male Wistar albino rats (200±20 gm, 5-week-old) were purchased from the experimental animal breeding farm (Helwan, Cairo, Egypt). The animals were maintained in a well-ventilated room under standard living conditions (25±2 ℃ temperature, 40–60% humidity,12-h dark/light cycle). During the study, a commercial solid pellet diet and tap water were made available for the rats, ad libitum. The experiment was conducted in the Anatomy Department, Faculty of Medicine, Benha University, Egypt. The study was performed in accordance with the scientific research ethics committee, Faculty of Medicine, Benha University, Egypt. During the experiment, the animals were managed and treated in accordance with the animal handling policy of Benha University's Faculty of Medicine and complies with the Guide for Care and Use of Laboratory Animals published by the US National Institutes of Health[12]. Ten-day-adaptation period was allowed for the animals before the start of the experiment. The rats were randomly divided into 7 groups, seven rats each: Control (received 2 mL/kg of the corresponding vehicle of each treatment (distilled water (2 rats); olive oil (2 rats); and normal saline containing ethanol 0.1% (3 rats), vit E, Melatonin, acrylamide alone, acrylamide/vit E, acrylamide/MT, and acrylamide/vit E/MT groups. All treatments were given via oral gavage for 8 weeks.

Blood and tissue sampling

At the end of the experiment, the abdomen was incised longitudinally under intramuscular xylazine-ketamine anesthesia and blood samples were obtained directly from the heart. Next, the anaesthetized rats were killed via cervical decapitation. The liver was dissected, removed, and washed with normal saline. Portions of the liver lobes were placed in 10% formaldehyde for histopathological examination. Other portions were stored at −20 °C for later biochemical analyses.

Biochemical analysis

The frozen liver tissue samples were collected in Ultra-Turrax homogenizer (IKA, Germany) and phosphate-buffered saline (PBS) was added, both were homogenized at 12000 rpm for 2 minutes in ice. The tissue homogenates were centrifuged (5000 x g for 30 min, at 4℃) and the supernatants were collected for measurements of Malondialdehyde (MDA) level, catalase (CAT), and superoxide dismutase (SOD) for evaluation of the lipid peroxidation and the oxidative status of the liver. The estimation of CAT (catalog #. EIACATC) and SOD (catalog #. EIASODC) activities was done by using commercially relevant kits based on the manufacturer's instructions (Thermofisher Scientific) and as previously stated by Aebi[13] and Sun *et al*.[14] respectively. Results were expressed as mmol/min/mg tissue. MDA was measured as described by Grotto *et al*.[15] following the manufacturer's protocol using the relevant kits (Abcam, catalog #. ab118970). Results were presented as nmol/mg tissue. From blood samples, alanine transaminase (ALT) (catalog #. TR71121), aspartate transaminase (AST) (catalog #. TR70121), and alkaline phosphatase (ALP) (catalog #. TR11320) levels were measured according to manufacturer's (Thermofisher Scientific) protocol.

Histological examination

The liver portions assigned for histopathological examination were fixed in 10% formol formalin solution for 2 days at room temperature, then dehydrated, cleared in xylol, infiltrated, and embedded in melted paraffin wax blocks. The prepared paraffin blocks were cut at 5 μm thickness, mounted on glass slides, then deparaffinized, hydrated in descending grades of ethanol and stained with hematoxylin and eosin and Masson trichrome according to Bancroft and Layton[16].

Immunohistochemical assay for detection of iNOS, Bax, and Bcl2 protein expression

Immunohistochemistry was performed to identify the protein expression of iNOS (inflammatory marker), Bax (pro-apoptotic marker), and Bcl2 (anti-apoptotic protein) for evaluation of the inflammatory status and pro-apoptotic/anti-apoptotic balance in the examined liver sections. For immunohistochemical (IHC) assay, 5 μm-cut-sections were mounted on positive charge glass slides, then deparaffinized, rehydrated, and cleared with xylol. The primary antibodies were rabbit polyclonal antibodies against iNOS, Bcl-2 (Lapvision corporation, catalog #: PA1-036, PA5-27094 respectively), and Bax (Sigma Aldrich, USA, catalog #: SAB4502549). Rabbit-specific HRP/DAB (ABC) detection IHC kits (Abcam, Cambridge, United Kingdom, Catalog #: ab64261) were used as secondary kits. The IHC technique was followed as described by Kiernan[17]. The sections were boiled in citrate buffer, pH 6 to retrieve antigen. The kits' hydrogen peroxide solution was used to block the endogenous peroxidase activity, then kit protein was blocked to minimize non-specific background staining. Each step was followed by PBS (pH 7.4) washing. The sections were incubated with the diluted primary antibody (1:500 for Bcl2, 1:200 for iNOS and Bax antibodies) in PBS for one hour. Biotinylated Goat secondary antibody was used and streptavidin peroxidase for another 30 min. The coloration was enhanced by using 3,3-diaminobenzidine (DAB) as a chromogen and hematoxylin solution for counterstaining. The positive reaction appeared as brownish cytoplasmic reaction. The positive controls for iNOS, Bcl2, and Bax were human heart, mouse spleen, and human lung cancer respectively. For the negative control, the step of the primary antibody was skipped. The stained slides were examined and photographed in the Anatomy Department, Faculty of Medicine, Benha University, Egypt. Nikon Eclipse 80i light microscope (Nikon Corporation, Japan) equipped with ToupCamTM Xcam full HD camera (ToupTek Europe, Ultramacro Ltd., UK) was used for visualization and photography purposes.

Morphometric study

Image analysis was performed by an expert blind to the study groups. JPG file format-photomicrographs were obtained by ToupCamTM Xcam digital camera and were subjected to image analysis using VideoTesT-Master (Morphology) software provided by Argussoft Ltd. company, Saint Petersburg, Russia. At magnification x200, the image analyzer was used for measurement of the area percent of collagen fibers, Bax, and Bcl2 immunostaining as well as the optical density of iNOS immunoexpression.

Statistical analysis

All research data were subjected to an initial check of normality and even distribution using Shapiro's test. One way ANOVA was used to detect significance followed by post hoc Tukey's test for comparison between the groups, using GraphPad Prism, Version 8 for Windows (San Diego, California, USA). The results were expressed as mean ± SD and statistical significance was considered at $P < 0.05$.

RESULTS

Biochemical findings

Biochemical analysis of the liver enzymes (Table 1) revealed a significant increase ($p<0.05$) in ALT, AST, and ALP in acrylamide (ACR)-exposed group when compared to control parameters. Separate treatment of either vit E or MT revealed a significant decrease ($p<0.05$) in the blood levels of liver enzymes when compared to ACR-exposed animals. Both vit E/MT combination resulted in a significant further decrease ($p<0.05$) with normalization of the measured liver enzymes.

Liver tissue homogenates analysis (Table 1) revealed an obvious increase ($p<0.05$) in MDA in the ACR-exposed rats when compared to the control group. Single and combined treatments showed a significant reduction ($p<0.05$), in relation to ACR group. The tissue levels of CAT and SOD were significantly decreased ($p<0.05$) in ACR group which were reversed ($p<0.05$) in the single and combined treatment with restoration of the control values in the combination group.

Light microscopic findings

Light microscopic examination of H & E-stained liver sections obtained from the control (Figures 1,2), vit E (Figure 3), melatonin (Figure 4)-treated groups showed normal hepatic organization. Hepatocytes were polyhedral in shape with acidophilic granular cytoplasm and were arranged in plates radiating from the central vein. The portal tracts were clearly seen and showed branches from the portal vein, hepatic artery, and bile duct (Figures 1,2,3,4). Hepatic blood sinusoids were lined by endothelial and Kupffer cells and were observed in-between the radiating plates (Figure 2). Acrylamide-exposed group showed disorganized hepatocyte plates marked by vacuolar degenerative changes mainly affecting the pericentral liver cells (Figure 5). Congested portal veins and detached endothelial lining cells of the central vein were frequent. Mononuclear cellular infiltration was observed in the portal area close to the congested portal vein (Figures 5,6). The affected hepatocytes showed cytoplasmic vacuolations and small condensed nuclei. The liver sinusoids were dilated and disarranged (Figure 7). ACR/Vit E CR

(Figure 8), ACR/MT (Figure 9), and ACR/Vit E/MT (Figure 10)-treated groups showed restoration of the hepatocyte plates organization. However, few cytoplasmic vacuoles were still observed in ACR/vit E-treated group (Figure 8).

Masson-stained liver sections of the control (Figure 11), vit E (Figure 12), melatonin (Figure 13)-treated groups showed normal fine collagen fibers distributed around central vein and periportal areas. Acrylamide group showed an extensive distribution of coarse collagen fibers in the portal area and the hepatic stroma (Figure 14). ACR/vit E-treated (Figure 15) and ACR/MT-treated (Figure 16) groups showed periportal localization of the collagen fibers. ACR/vit E/MT group showed seemingly normal distribution of fine delicate collagen fibers like control (Figure 17).

Immunohistochemical observations

Anti-Bax immunohistochemical assay of liver sections in the control (Figure 18), vit E (Figure 19), and melatonin (Figure 20)-treated groups showed a negative anti-Bax immunoreaction. However, the acrylamide-exposed group showed a diffuse positive anti-Bax immunoreaction, markedly prominent in the hepatocyte's cytoplasm and the limiting boundaries of the liver blood sinusoids (Figure 21). ACR/vit E (Figure 22) and ACR/MT (Figure 23)-treated groups showed a moderate decrease in the Bax immunoreactivity. Meanwhile, the ACR/vit E/MT-treated group displayed a very mild anti-Bax immunoreactivity restricted to the limiting boundaries of hepatic blood sinusoids (Figure 24).

On the other hand, anti-Bcl2 immunohistochemical assay of the control (Figure 25), vit E (Figure 26), and melatonin (Figure 27)-treated groups demonstrated a widely distributed strong positive hepatocytes cytoplasmic immunoreaction. Meanwhile, the acrylamide-exposed group (Figure 28) showed very minimal Bcl2 immunoreactivity. ACR/vit E (Figure 29), ACR/MT (Figure 30), and ACR/vit E/MT (Figure 31)-treated groups revealed a moderate increase in the Bcl2 immunostaining.

The anti-iNOS immunohistochemical assay viewed a negative anti-iNOS immunoreaction in the control (Figure 32), vit E (Figure 33), and melatonin (Figure 34)-treated groups. Acrylamide-exposed group (Figure 35) showed a diffuse intense iNOS immunostaining in hepatocytes cytoplasm. ACR/vit E (Figure 36) and ACR/MT (Figure 37)-treated groups revealed less intense immunoreactivity. However, ACR/Vit E/MT-treated group showed hepatocytes with partial resolve of the anti-iNOS immunoreaction (Figure 38).

Morphometric result

The morphometric measurements of the area percent of collagen fibers distribution, Bax, Bcl2 immunostaining and the optical density of iNOS immunoexpression were shown in (Figure 39). The control, vit E, and melatonin alone-treated groups showed a non-significant change when compared to each other. In comparison with the control group, the acrylamide-exposed group displayed a significant increase ($p<0.05$) in the mean iNOS optical density and the mean area percent of masson-stained collagen fibers and Bax immunoreactivity, meanwhile a significant decrease ($p<0.05$) in Bcl2 immunoexpression was noted. Either vit E or MT treatment resulted in a significant reversal ($p<0.05$) of the altered parameters with complete improvement in the combination group, when compared to the control animal group.
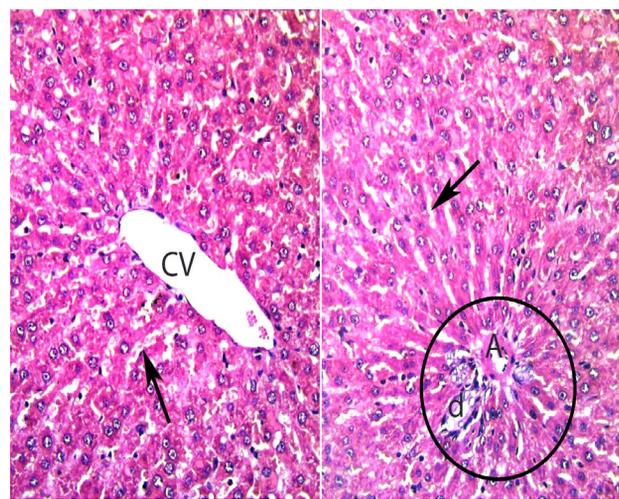
Fig. 1: H & E-stained photomicrographs of a liver section in the control group (magnification x200) showing normal hepatic architecture. The liver cells are arranged in radiating plates with intervened hepatic blood sinusoids (arrows) draining into the central vein (CV). The portal area (circle) is seen containing branches of the hepatic artery (A) and bile ducts (d).
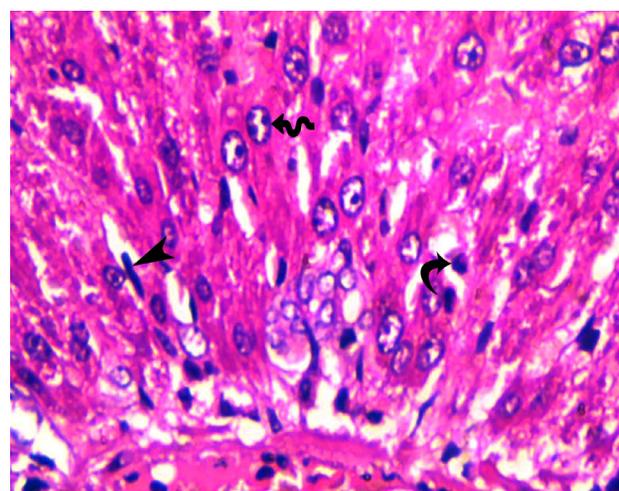
Fig. 2: High magnification (x400) of H & E-stained control liver section showing hepatocytes arrangement in plates with acidophilic granular cytoplasm and vesicular nuclei (zigzag arrow). Endothelial cells (arrowheads) and Kupffer cells (curved arrows) are seen lining the blood sinusoids.
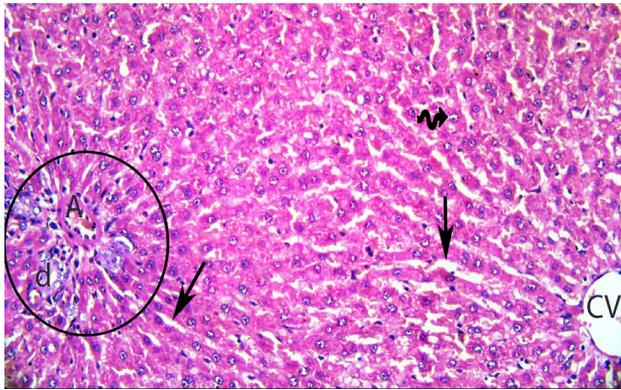
Fig. 3: H & E-stained photomicrograph of a liver section in the vit E group (magnification x200) showing normal hepatic architecture. The central vein (CV) is seen draining the blood sinusoids (arrows). The portal tract (marked by circle) is seen containing branches of the hepatic artery (A) and a bile duct (d). The hepatocytes are acidophilic and granular with vesicular nuclei (zigzag arrow) and are organized in radiating cords or plates.

Fig. 4: H & E-stained photomicrographs of a liver section in melatonin group (magnification x200) showing normal hepatic architecture. The hepatocytes appear acidophilic with vesicular nuclei (zigzag arrow) and placed in plates radiating from the central vein (CV). The portal area is seen containing branches of the portal vein (PV). The hepatic blood sinusoids (arrows) are also seen traversing through the hepatocyte's plates.

Fig. 5: H & E-stained photomicrograph of a liver section in the acrylamide-exposed group (magnification x200) showing disorganized hepatocyte plates with vacuolated cytoplasm (U-shaped arrows). The central vein (CV) shows detached endothelial cell lining (arrowheads).

Fig. 6: H & E-stained photomicrograph of a liver section in the acrylamide-exposed group (magnification x200) showing mononuclear inflammatory cell infiltrates (stars) close to the congested portal vein (PV).

Fig. 7: High magnification (x400) of H & E-stained liver section in acrylamide-exposed group showing disorganized hepatocytes showing cytoplasmic vacuoles (U-shaped arrows). Some hepatocytes show small dark nuclei (arrows with tails). The liver blood sinusoids (arrows) are disarranged and dilated.

Fig. 8: H & E-stained photomicrograph of a liver section in the acrylamide/vit E-treated group (magnification x200) showing reorganization of the hepatocyte plate arrangement around the central vein (CV). Less abundant cytoplasmic vacuolation (U-shaped arrows) are still present.
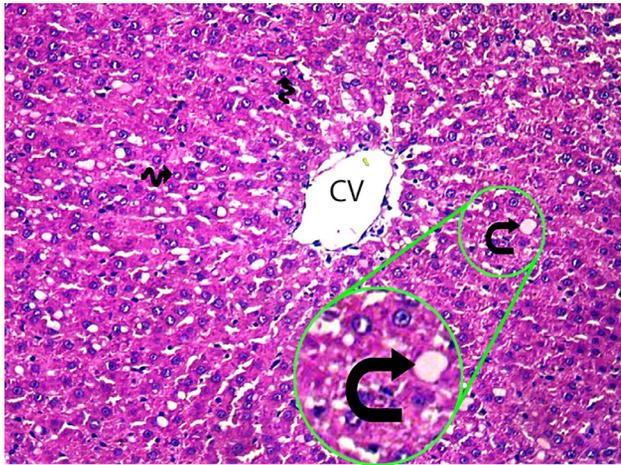
Fig. 9: H & E-stained photomicrograph of a liver section in the acrylamide/melatonin-treated group (magnification x200) showing an improved histological structure of the liver with very few vacuolar changes (U-shaped arrows). The liver cells appear acidophilic with vesicular nuclei (zigzag arrows) radiating from the central vein (CV).
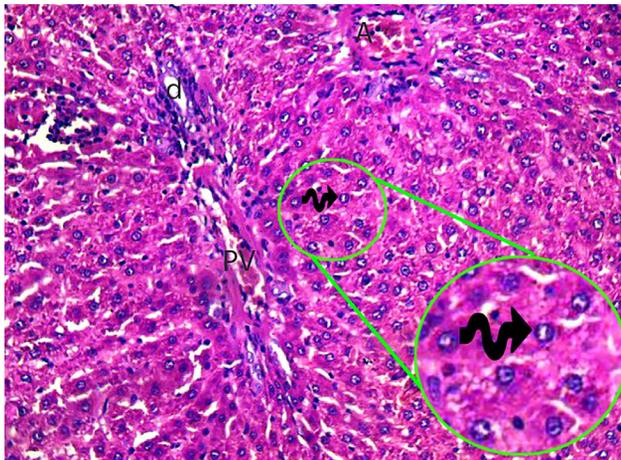
Fig. 10: H & E-stained photomicrograph of a liver section in the acrylamide/vit E/melatonin-treated group (magnification x200) showing restoration of the hepatic microstructure. Hepatocytes show acidophilic granular cytoplasm with vesicular nuclei (zigzag arrow). The portal tract is seen containing branches of the Hepatic artery (A), portal vein (PV), and bile duct (d).
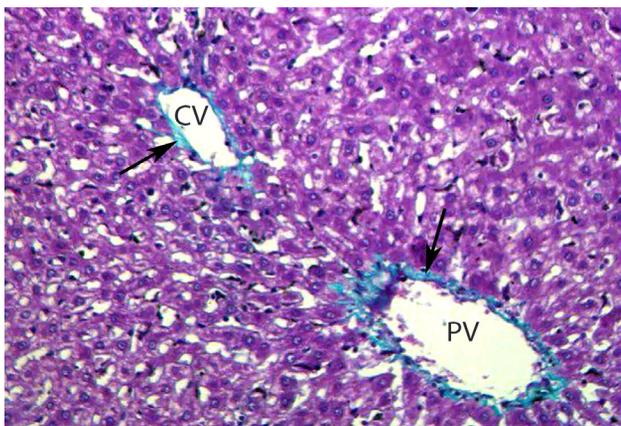
Fig. 11: Masson-stained photomicrograph of a liver section in the control group (magnification x200) showing pericentral (CV) and periportal (PV) distribution of normal, green-colored delicate collagen fibers (arrows).
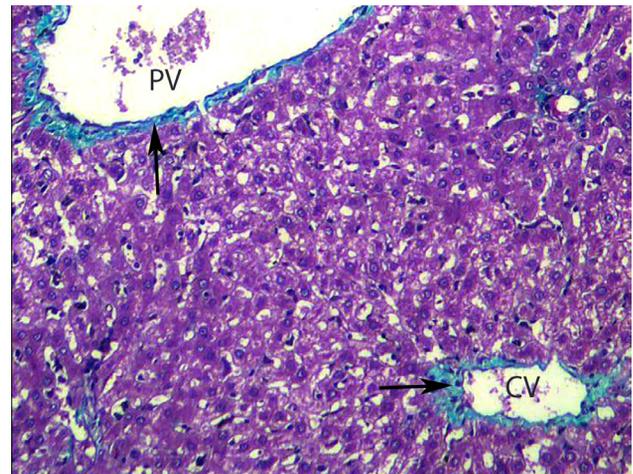
Fig. 12: Masson-stained photomicrograph of a liver section in the vit E group (magnification x200) showing the normal pericentral (CV) and periportal (PV) distribution of delicate collagen fibers (arrows).
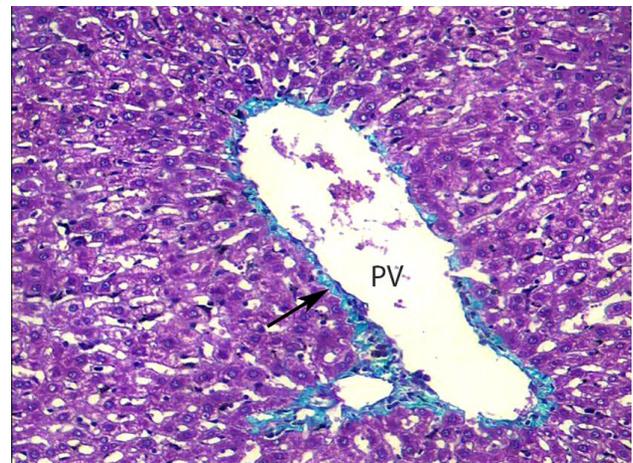
Fig. 13: Masson-stained photomicrograph of a liver section in the melatonin group (magnification x200) showing the normal periportal (PV) distribution of delicate collagen fibers (arrow).
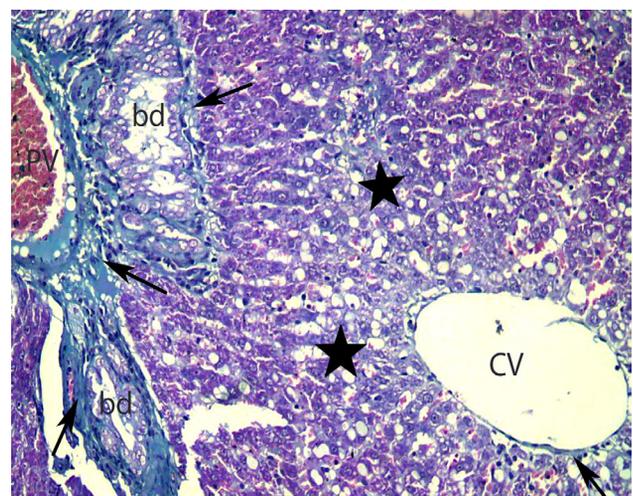
Fig. 14: Masson-stained photomicrograph of a liver section in the acrylamide-exposed group (magnification x200) showing extensively distributed coarse collagen fibers in portal area around portal vein (PV) and bile ducts (bd) (arrows) and in the background stroma of the vacuolated hepatocytes (stars) around central vein (CV).
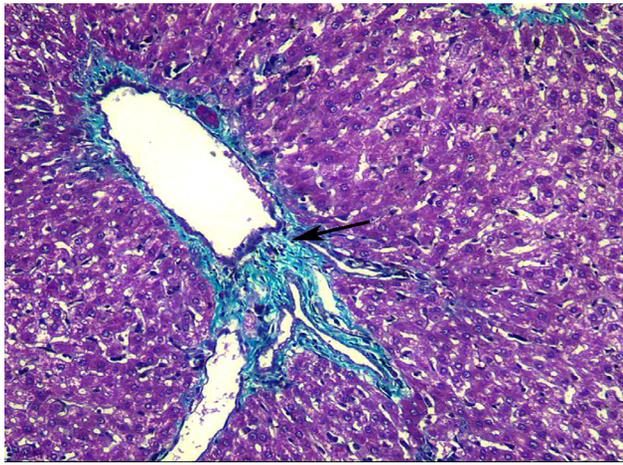
Fig. 15: Masson-stained photomicrograph of a liver section in the ACR/vit E-treated group (magnification x200) showing periportal localization of coarse collagen fibers.

Fig. 16: Masson-stained photomicrograph of a liver section in the ACR/MT-treated group (magnification x200) showing coarse collagen fibers (arrows) located around portal area (marked by its contents, portal vein (PV) and hepatic artery (HA).

Fig. 17: Masson-stained photomicrograph of a liver section in the acrylamide/vit E/MT-treated group (magnification x200) showing apparently normal distribution and intensity of delicate collagen fibers (arrows) around central vein (CV).

Fig. 18: Anti-Bax immunoassay photomicrograph in the control group (magnification x400) showing negative anti-Bax immunoreaction.

Fig. 19: Anti-Bax immunoassay photomicrograph in the vit E group (magnification x400) showing negative anti-Bax immunoreaction.
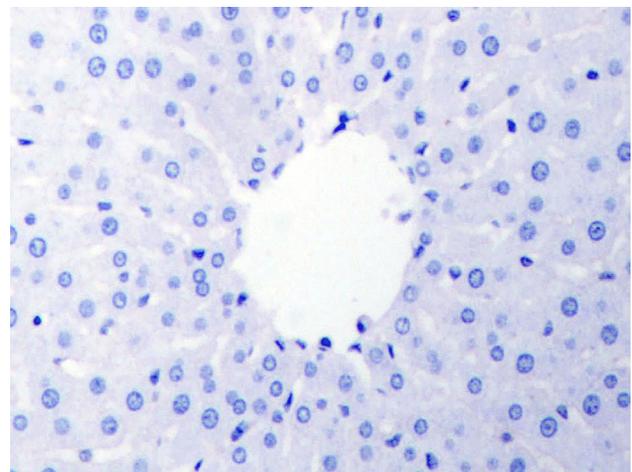
Fig. 20: Anti-Bax immunoassay photomicrograph in the melatonin group (magnification x400) showing negative anti-Bax immunoreaction.
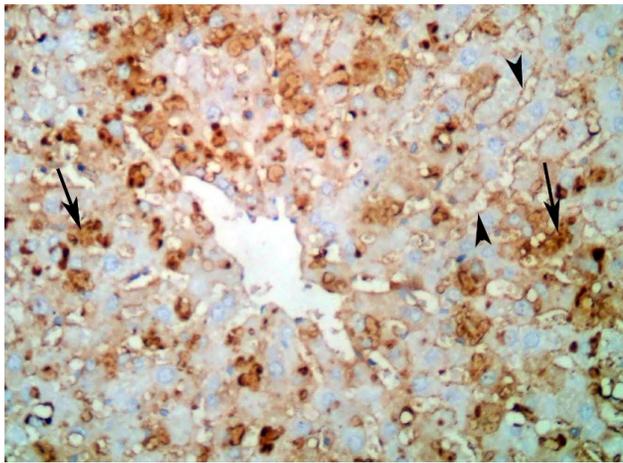
Fig. 21: Anti-Bax immunoassay photomicrograph in the acrylamide-exposed group (magnification x400) showing hepatocytes with strong positive reaction staining the cytoplasm (arrows) and the limiting boundaries of hepatic blood sinusoids (arrowheads).
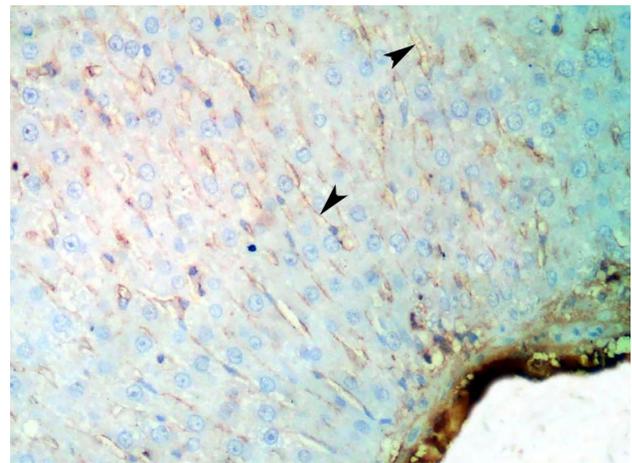
Fig. 24: Anti-Bax immunoassay photomicrograph in the acrylamide/vit E/MT-treated group (magnification x400) showing very mild anti-Bax immunoreactivity limited to the boundaries of the hepatic blood sinusoids (arrowheads).
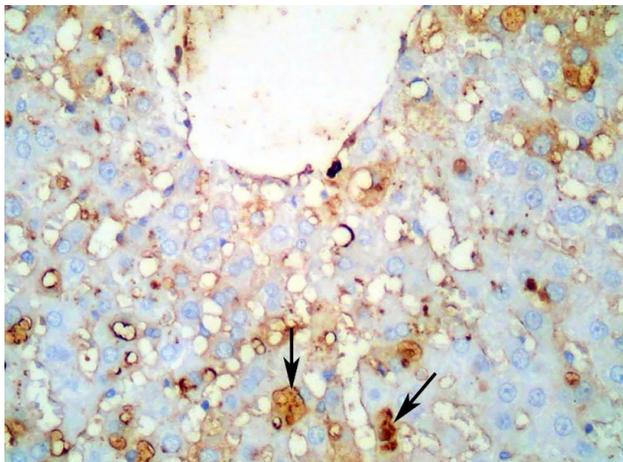
Fig. 22: Anti-Bax immunoassay photomicrograph in the acrylamide/ vit E-treated group (magnification x400) showing positive anti-Bax immunoreaction (arrows) with a moderate decrease in the intensity and distribution of the immunoreaction.
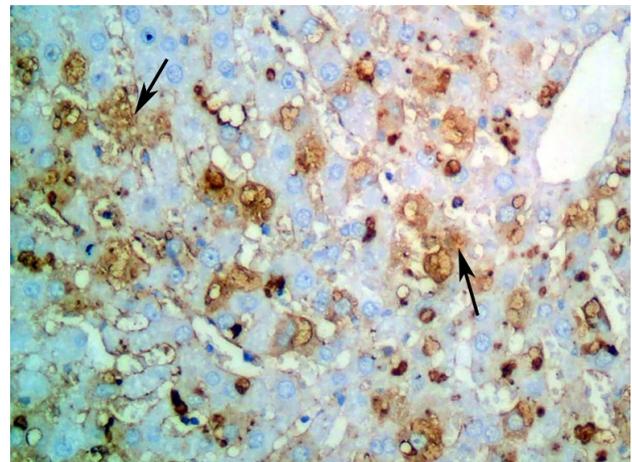
Fig. 25: Anti-Bcl2 immunohistochemical assay of a liver section in the control group (magnification x400) showing diffuse strong positive hepatocytes cytoplasmic immunoreaction (arrows).
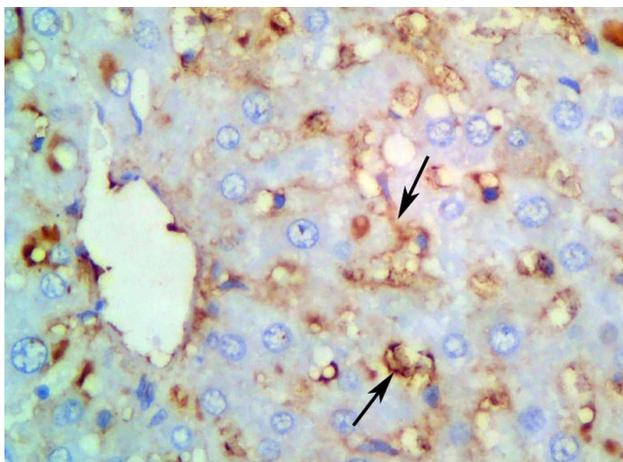
Fig. 23: Anti-Bax immunoassay photomicrograph in the acrylamide/ MT-treated group (magnification x400) showing positive anti-Bax immunoreaction (arrows) with a remarkable decrease in the intensity and distribution of the immunoreaction.
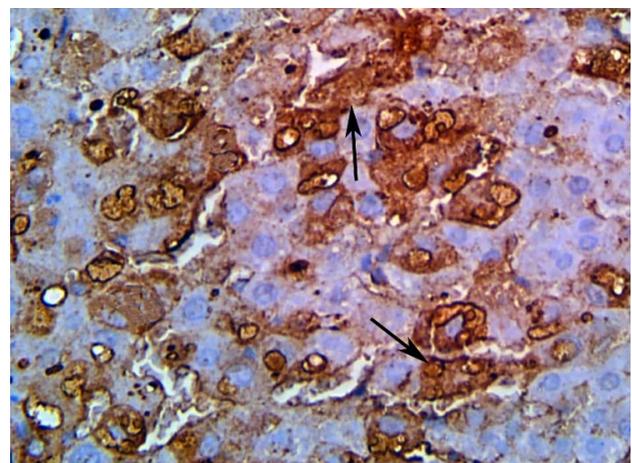
Fig. 26: Anti-Bcl2 immunohistochemical assay of a liver section in the vit E group (magnification x400) showing diffuse strong positive hepatocytes cytoplasmic immunoreaction (arrows).
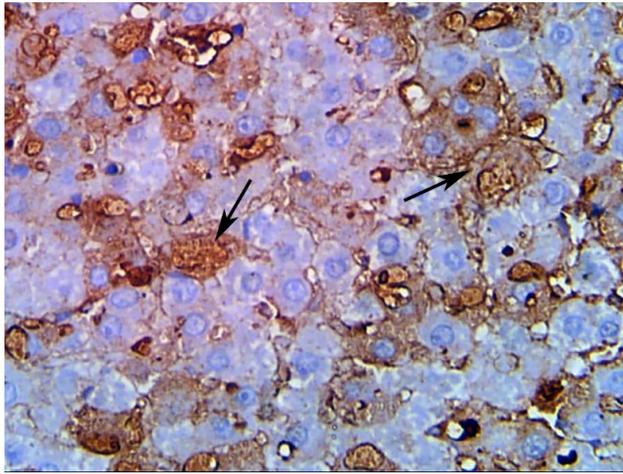
Fig. 27: Anti-Bcl2 immunohistochemical assay of a liver section in the melatonin group (magnification x400) showing diffuse strong positive hepatocytes cytoplasmic immunoreaction (arrows).
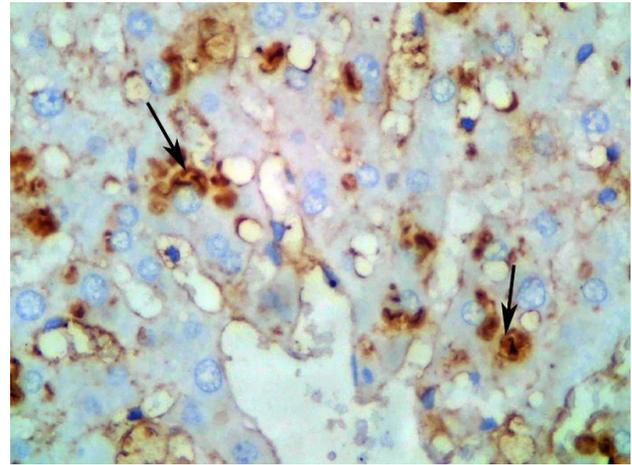
Fig. 30: Anti-Bcl2 immunohistochemical assay of a liver section in the acrylamide/melatonin-treated group (magnification x400) showing a moderate increase in the Bcl2 immunostaining (arrows).
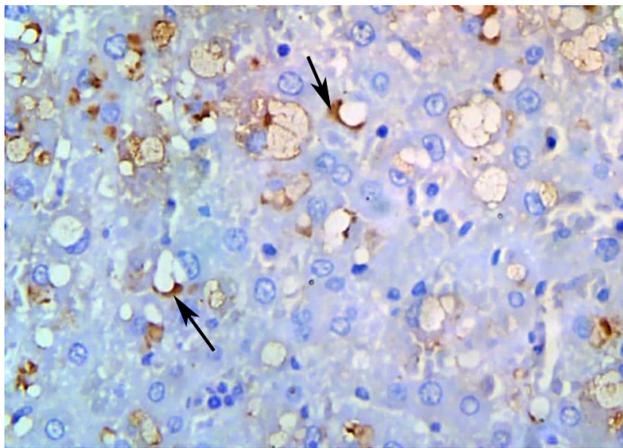
Fig. 28: Anti-Bcl2 immunohistochemical assay of a liver section in the acrylamide-exposed group (magnification x400) showing very minimal Bcl2 immunoreactivity (arrows).
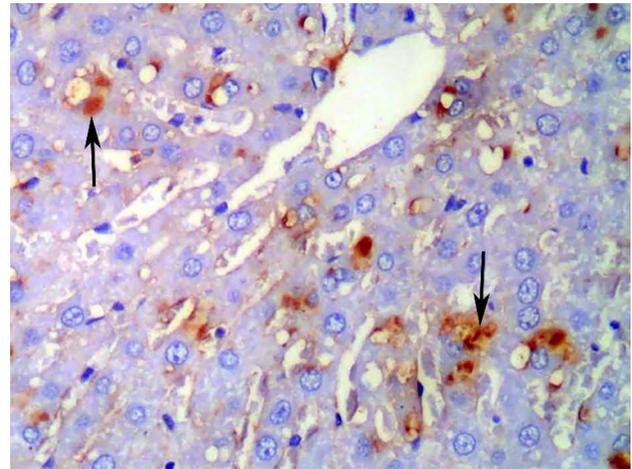
Fig. 31: Anti-Bcl2 immunohistochemical assay of a liver section in the acrylamide/vit E/MT-treated group showing a moderate increase in the Bcl2 immunoreaction (arrows).
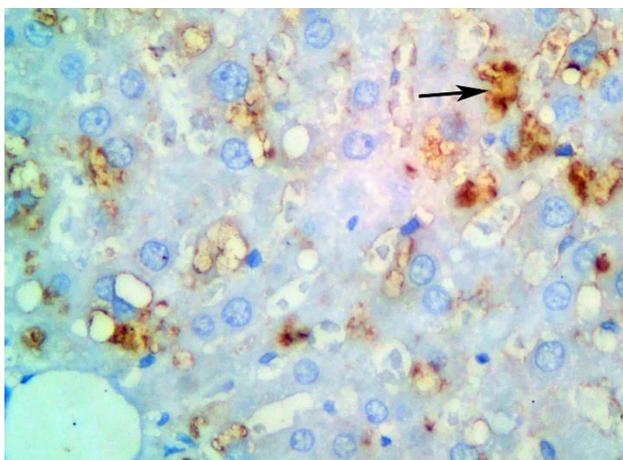
Fig. 29: Anti-Bcl2 immunohistochemical assay of a liver section in the acrylamide/vit E-treated group (magnification x400) showing a mild increase in the Bcl2 immunostaining (arrow).
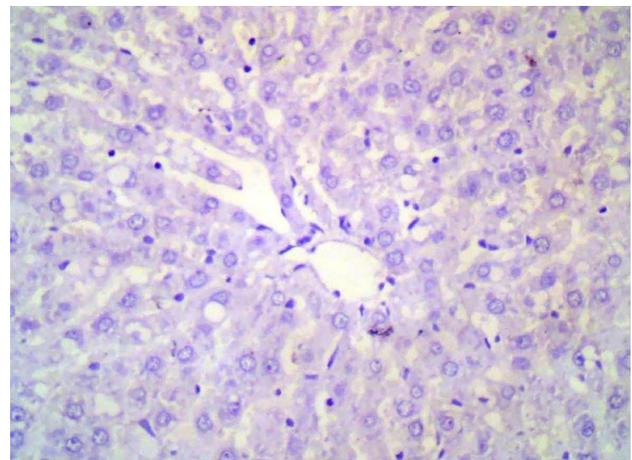
Fig. 32: Anti-iNOS immunohistochemical assay of a liver section in the control group (magnification x400) showing negative anti-iNOS immunoreaction.
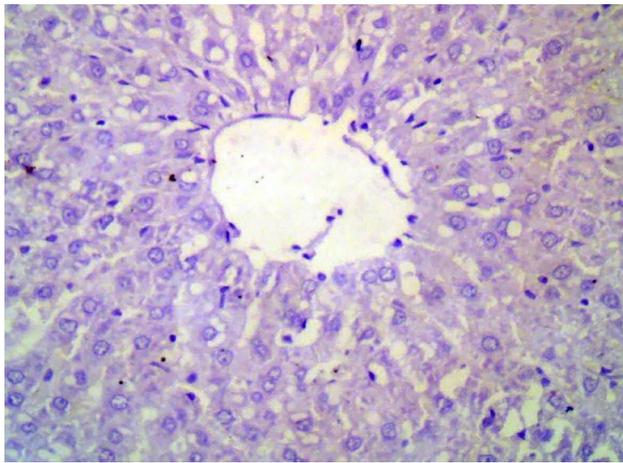
Fig. 33: Anti-iNOS immunohistochemical assay of a liver section in the vit E group (magnification x400) showing negative anti-iNOS immunoreaction.
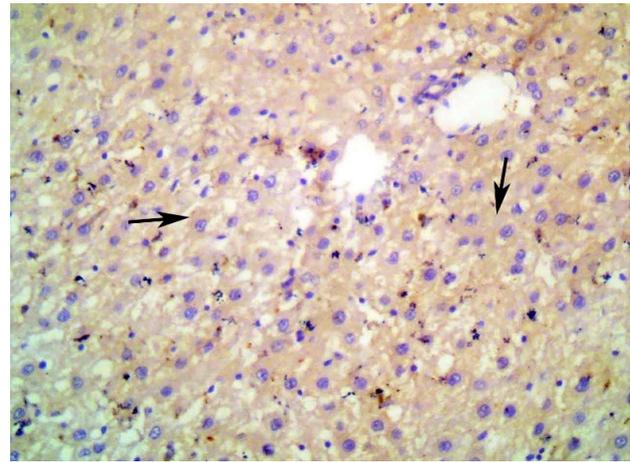
Fig. 36: Anti-iNOS immunohistochemical assay of a liver section in the acrylamide/vit E group (magnification x400) showing diffuse less intense positive hepatocyte cytoplasmic immunoreaction (arrows).
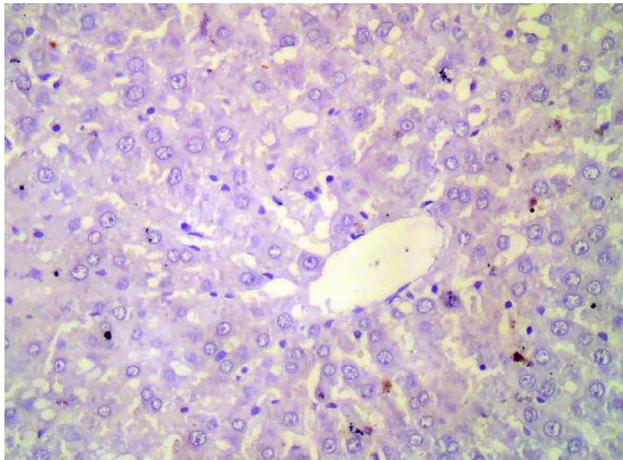
Fig. 34: Anti-iNOS immunohistochemical assay of a liver section in the melatonin group (magnification x400) showing negative anti-iNOS immunoreaction.
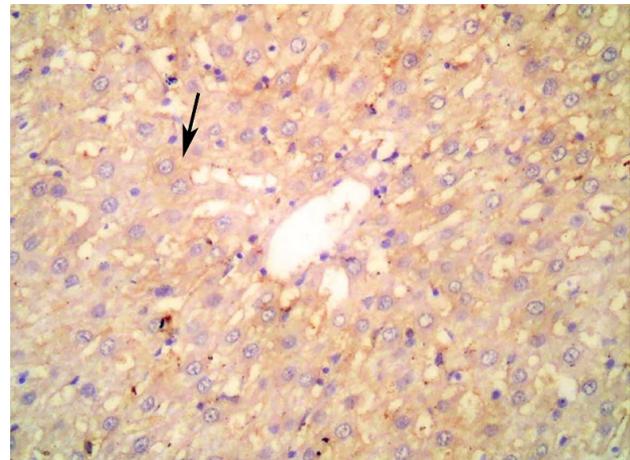
Fig. 37: Anti-iNOS immunohistochemical assay of a liver section in the acrylamide/MT-treated group (magnification x400) showing diffuse less intense positive hepatocyte cytoplasmic immunoreaction (arrow).
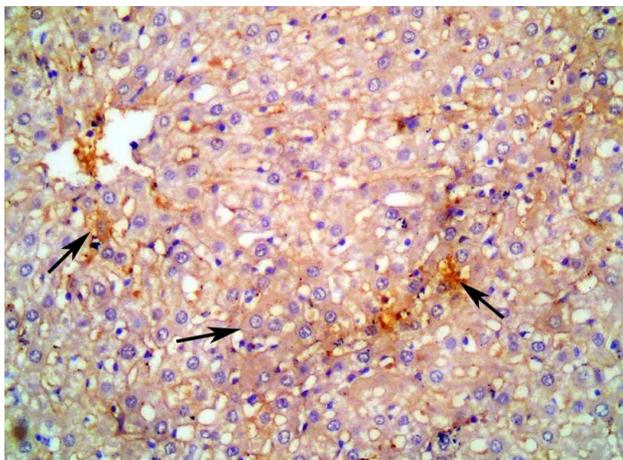
Fig. 35: Anti-iNOS immunohistochemical assay of liver sections in the acrylamide-exposed group (magnification x400) showing diffuse strong positive hepatocyte cytoplasmic immunoreaction (arrows).
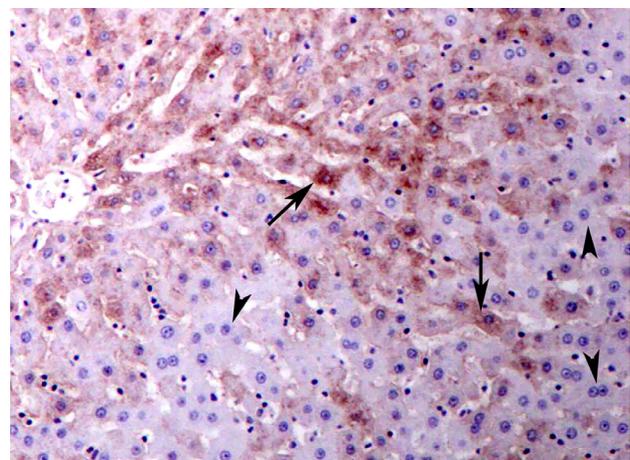
Fig. 38: Anti-iNOS immunohistochemical assay of a liver section in the acrylamide/vit E/MT-treated group (magnification x400) showing some hepatocytes with positive hepatocyte cytoplasmic immunoreaction (arrows), however many others showed a remarkable resolve of the iNOS-immunoreactivity (arrowheads).
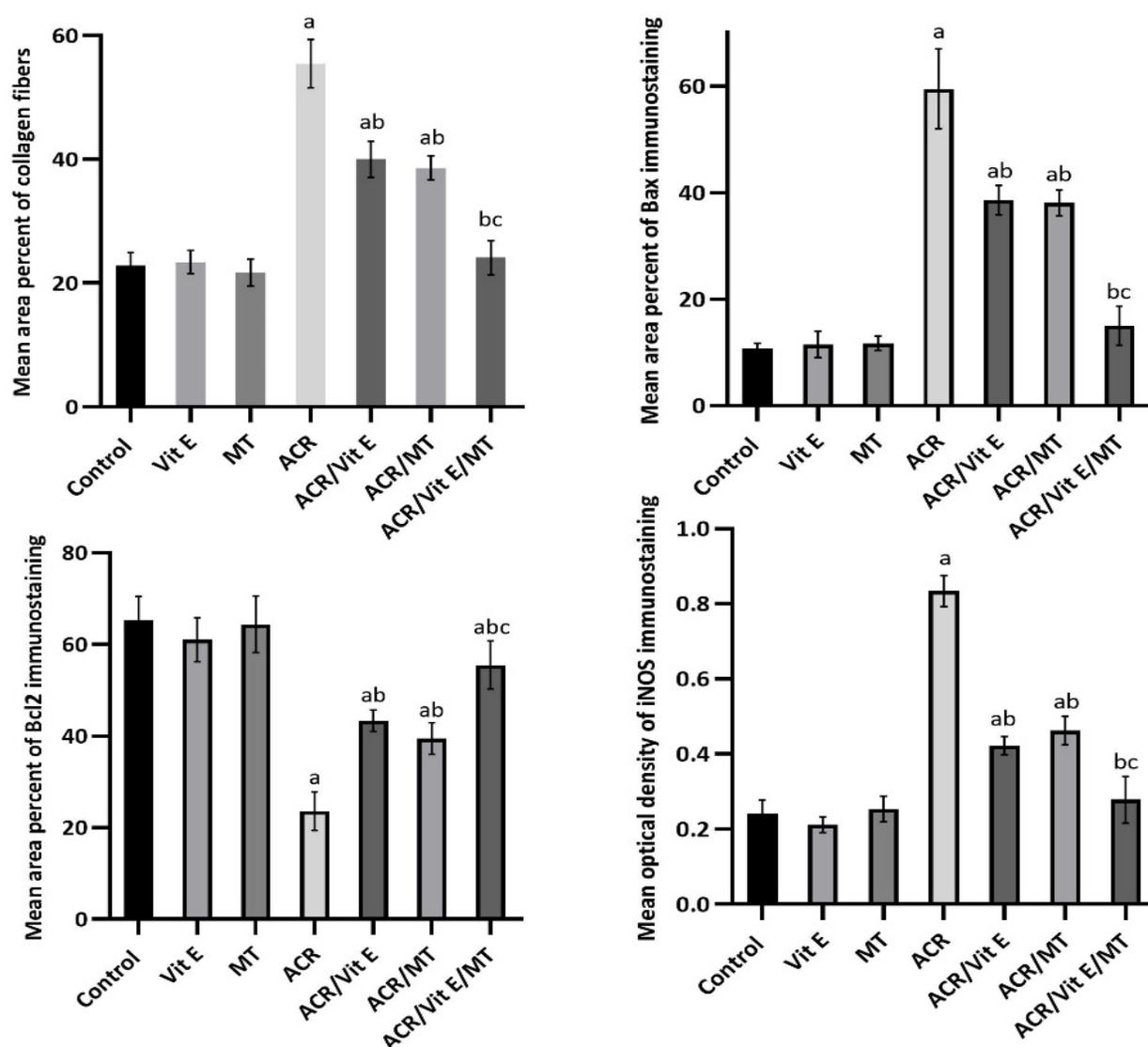
Fig. 39: Effect of vit E and or melatonin on the mean area percent of collagen fiber, Bax, Bcl2 immunoreactivities and the mean optical density of iNOS immunostaining. The findings are expressed as mean ± SD. a significant versus control, Vit E, and MT. b significant versus ACR group. c significant versus ACR/Vit E & ACR/MT groups. One-way ANOVA followed by Post hoc Tukey's test for comparison between groups was used. Statistical significance was considered at $p<0.05$.

Table 1: The effect of vitamin E and or melatonin on serum levels of liver enzymes and liver tissue concentrations of the oxidative/ antioxidative parameters

	Control	Vit E	MT	ACR	ACR/Vit E	ACR/MT	ACR/Vit E+MT
ALT (U/L)	75.13±9.27	73.96±10.01	76±8.78	97.98±7.56[a]	80.45±8[ab]	79.54±9.5[b]	74.34±9.67[b]
AST (U/L)	101.28±15.56	97.48±10.56	98.34±9.04	205.78±18.27[a]	170.67±12.78[ab]	=150.63±14.34[abc]	115.22±12.7[bd]
ALP(U/L)	135.23±9.7	137.09±10	134.17±11.1	249.56±15.68[a]	154.23±8.7ab	144.24±9.3[abc]	129±8.98 bd
MDA (nmol/mg)	40.9±3.21	37.65±2.5	42.16±3.56	95±8.71[a]	71.54±7.71[ab]	60.23±6.05[abc]	48,87±5.34[abd]
CAT (mmol/min/mg)	32.79±1.5	29±2.67	33.65±3	14.01±0.97[a]	21.91±4.09[ab]	27.2±2.63[abc]	33.3±3.4[bd]
SOD (mmol/min/mg t)	25.11±3.7	24.45±5.78	27.25±3.8	8.89±3.78[a]	14±2.89[b]	20.23±3[abc]	26.39±4.6[bd]

The value of each group is presented as mean±SD. a significant vs control group, b significant vs acrylamide (ACR) group, c significant vs ACR/vitamin E (vit E) group and d significant vs ACR/vit E and ACR/melatonin (MT) groups. One-way ANOVA was used followed by Tukey's post hoc test for groups' comparison at $P < 0.05$.

DISCUSSION

The present study investigated the effect of 2 natural agents, vitamin E and melatonin on acrylamide (ACR)-induced liver injury in adult male albino rats. Although their separate curative potential, in different organs with other toxicities, has been reported in the literary data, this work investigated both vit E and melatonin in combination. The results confirmed the toxic effect of ACR on the rat liver when given orally at a dose of 5 mg/kg for 8 weeks. Moreover, the study showed an ameliorative effect of Vit E and melatonin (MT) on such liver damage by regulating iNOS, Bax, and Bcl2 expressions and resetting collagen synthesis and turnover, hence anti-inflammatory, anti-apoptotic, antifibrotic mechanisms.

The control, vit E, and MT alone-treated groups showed the same biochemical, histological, and immunohistochemical findings. (ACR) exposure resulted in major changes in the biochemical analyses and hepatic histoarchitecture. ACR significantly elevated the liver enzymes when compared to the control group. Also, disorganization of the hepatic histoarchitecture, hepatic vascular congestion, and cellular infiltrates were the major findings in H & E staining. Similarly, Hamdy *et al.*[10] reported biochemical and histological liver affection in the same rat model of ACR-induced liver injury. Taking into account the elevated liver enzymes in correlation with imbalanced SOD/MDA in liver tissues, the authors could suggest hepatocytes' inflammatory and oxidative stress as a reason for the H & E changes and iNOS, Bax, Bcl2 immunohistochemical alterations leading to elevation of ALT, and AST. Histomorphometric evaluation of the immunohistochemical assays could imply an upregulation of pro-apoptotic proteins (Bax) and pro-inflammatory mediators (iNOS) and down-regulation of anti-apoptotic proteins (Bcl2) as mechanistic aspects for ACR-induced liver damage. In accordance, Guo *et al.*[18] reported pro-inflammatory status and upregulation of apoptosis in a rat model of ACR-induced neurotoxicity.

Evaluation of the Mallory-stained liver sections displayed an accumulation of collagen fibers in ACR-intoxicated rats. The authors assumed hepatic stellate cells (HSCs) activation (not investigated herein) facilitated by the inflammatory and oxidative stress microenvironment with subsequent myofibroblast transformation and excess fibrous tissue formation. The authors' suggestion was emphasized by the findings of Shaker *et al.*[19] who reported TNF-α/IL-6-mediated HSCs activation in a rat model of thioacetamide-induced hepatic fibrosis.

Either vitamin E-alone or MT-alone treatment in ACR-exposed rats led to a significant improvement in the biochemical and histological alterations of the liver, however still mild degenerative hepatocyte changes were observed in ACR/vit E-treated rats. These results were consistent with other studies focusing on the protective potential of vit E and melatonin. Several studies have reported counteraction of ACR-induced toxicity by vit

E in different organ toxicities e.g. striated muscles[20], fetal liver[21], and testis[22]. Moreover, Oleshchuk *et al.*[23] confirmed a hepatoprotective effect for melatonin on a rat model of carbon tetrachloride (CCl4)-induced liver injury.

The reversal of oxidant/antioxidant imbalance in the liver tissue by both vit E and melatonin might ameliorate the hepatic histoarchitecture and cellular functions with a decrease in liver enzymes. Actually, both agents' treatment decreased MDA, and increased catalase/SOD concentrations in liver, coupled with a decrease in liver enzymes. Parallel, Bicer *et al.*[24] and Kopańska *et al.*[25] reported antioxidant and anti-inflammatory effects for melatonin and α-tocopherol in different animal modeling. Hence, the anti-inflammatory, and antioxidant capabilities of melatonin and tocopherol might be an explanation for the improved histological and biochemical findings in both agents treated groups. The counteraction to apoptosis, exerted by tocopherol and MT could be attributed to the downregulation of pro-apoptotic Bax and upregulation of anti-apoptotic protein, Bcl2. Also, the downregulated iNOS immunoexpression exerted by tocopherol and melatonin might be correlated with interference with Bax expression. This assumption was coincident with the finding of Famurewa *et al.*[26] who reported iNOS/NF-κB/caspase-3 signaling downregulation mediated by zinc treatment in a rat model of cyclophosphamide-induced cystitis.

In the authors' regard, the subsidence of the inflammatory and oxidative status and hence, possible HSCs inactivation might explain the decreased amount of collagen in Mallory-stained sections of the tocopherol- and melatonin-treated groups. This notion was supported by Hamid *et al.*[27] who reported amelioration of inflammation and oxidative stress and HSCs inactivation by selenized Astragalus polysaccharides in a rat model of CCl4-induced liver injury.

In vit E/MT combination group, the hepatic structural organization was restored which was in harmony with the improved liver enzymes and the reestablished oxidative balance. Morphometric evaluation of the immunoassay slides confirmed better findings than in single treatment groups. These findings referred to summative actions of both vit E and MT combined due to the further addition of the antioxidant and anti-inflammatory effects as confirmed by the remarkable amelioration of inflammation/oxidative stress biomarkers. Similarly, Erdemli *et al.*[28] reported a synergistic action of both vit E/MT combination in a mouse model of pesticide-induced nephrotoxicity.

CONCLUSION

Acrylamide hepatotoxicity was proven in the current rat model of acrylamide exposure. The histopathological and biochemical findings referred to a significant alteration in the hepatic tissues, leading to precipitation of inflammation and oxidative stress. Single tocopherol and melatonin treatment exhibited robust antioxidant and anti-inflammatory effects. Co-administration of both exhibited more powerful synergistic effects coupled with

the increased antioxidant capacity. Hence, the Vit E/ MT combined administration is recommended as a daily supplement, in particular, for those who are exposed to acrylamide e.g. fast food-lovers.

CONFLICT OF INTERESTS

There are no conflicts of interest.

REFERENCES

1. Quesada-Valverde M, Artavia G, Granados-Chinchilla F, Cortés-Herrera C. Acrylamide in foods: from regulation and registered levels to chromatographic analysis, nutritional relevance, exposure, mitigation approaches, and health effects. Toxin Rev 2022:1–31. https://doi.org/10.1080/15569543.2021.2018611

2. Elhelaly AE, AlBasher G, Alfarraj S, Almeer R, Bahbah EI, Fouda M, Bungău SG, Aleya L, Abdel-Daim MM. Protective effects of hesperidin and diosmin against acrylamide-induced liver, kidney, and brain oxidative damage in rats. Environ Sci Pollut Res 2019; 26:35151–35162. https://doi.org/10.1007/s11356-019-06660-3

3. Rifai L, Saleh FA. A review on acrylamide in food: Occurrence, toxicity, and mitigation strategies. Int J Toxicol 2020; 39:93–102. https://doi.org/10.1177/1091581820902405

4. Miazek K, Beton K, Śliwińska A, Brożek-Płuska B. The Effect of β-Carotene, Tocopherols and Ascorbic Acid as Anti-Oxidant Molecules on Human and Animal In *Vitro*/In *Vivo* Studies: A Review of Research Design and Analytical Techniques Used. Biomol 2022; 12. https://doi.org/10.3390/biom12081087

5. Cuce G, Çetinkaya S, Koc T, Esen HH, Limandal C, Balcı T, Kalkan S, Akoz M. Chemoprotective effect of vitamin E in cyclophosphamide-induced hepatotoxicity in rats. Chem Biol Interact 2015; 232:7–11. https://doi.org/10.1016/j.cbi.2015.02.016

6. Chalouati H, Ben Sâad MM, Payrastre L. Hepatoprotective effects of vitamin E against hexachlorobenzene-induced hepatotoxicity and oxidative stress in rats: histological, biochimical and antioxidant status changes. Toxicol Mech Methods 2019; 29:18–25. https://doi.org/10.1080/15376516.2018.1506847

7. Alahmadi BA, El-Alfy SH, Hemaid AM, Abdel-Nabi IM. The protective effects of vitamin E against selenium-induced oxidative damage and hepatotoxicity in rats. J Taibah Univ Sci 2020; 14:709–720. DOI:10.1080/16583655.2020.1769256

8. Samanta S. Physiological and pharmacological perspectives of melatonin. Arch Physiol Biochem 2020:1–22. https://doi.org/10.1080/13813455.2020.1770799

9. Bantounou M, Plascevic J, Galley HF. Melatonin and Related Compounds: Antioxidant and Anti-Inflammatory Actions. Antioxidants 2022; 11. https://doi.org/10.3390/antiox11030532

10. Hamdy SM, El-Khayat Z, Farrag AR, Sayed ON, El-Sayed MM, Massoud D. Hepatoprotective effect of Raspberry ketone and white tea against acrylamide-induced toxicity in rats. Drug Chem Toxicol 2022; 45:722–730. https://doi.org/10.1080/01480545.2020.1772279

11. Yang Z, He Y, Wang H, Zhang Q. Protective effect of melatonin against chronic cadmium-induced hepatotoxicity by suppressing oxidative stress, inflammation, and apoptosis in mice. Ecotoxicol Environ Saf 2021; 228:112947. https://doi.org/10.1016/j.ecoenv.2021.112947

12. NIH. Guide for the Care and Use of Laboratory Animals. 8th ed. New York, USA: National Academies Press (US); 2011. https://doi.org/10.1038/s41684-021-00871-3

13. Aebi H. [13] Catalase in *vitro*. Methods Enzymol 1984; 105:121–126. doi: 10.1016/s0076-6879(84)05016-3

14. Sun YI, Oberley LW, Li Y. A simple method for clinical assay of superoxide dismutase. Clin Chem 1988; 34:497–500. PMID: 3349599

15. Grotto D, Maria LS, Valentini J, Paniz C, Schmitt G, Garcia SC, Pomblum VJ, Rocha JBT, Farina M. Importance of the lipid peroxidation biomarkers and methodological aspects for malondialdehyde quantification. Quim Nova 2009; 32:169–174. https://doi.org/10.1590/s0100-40422009000100032

16. Bancroft JD, Layton C. The Hematoxylins and Eosin /Connective and other mesenchymal tissues with their stains. In: Suvarna KS, Layton C, Bancroft JD (eds.), Bancroft's theory and practice of histological techniques E-Book. 8th ed. Elsevier Health Sciences; 2019.

17. Kiernan JA. Immunohistochemistry. In: Kiernan J (ed.), Histological and histochemical methods. Theory and practice. 4th-th ed. Scion Publishing Ltd; 2015:454–490.

18. Guo J, Cao X, Hu X, Li S, Wang J. The anti-apoptotic, antioxidant and anti-inflammatory effects of curcumin on acrylamide-induced neurotoxicity in rats. BMC Pharmacol Toxicol 2020; 21:1–10. https://doi.org/10.1186/s40360-020-00440-3

19. Shaker ME, Eisa NH, Elgaml A, El-Mesery A, El-Shafey M, El-Dosoky M, El-Mowafy M, El-Mesery M. Ingestion of mannose ameliorates thioacetamide-induced intrahepatic oxidative stress, inflammation and fibrosis in rats. Life Sci 2021; 286:120040. https://doi.org/10.1016/j.lfs.2021.120040

20. Al-Serwi RH, Ghoneim FM. The impact of vitamin E against acrylamide induced toxicity on skeletal muscles of adult male albino rat tongue: Light and electron microscopic study. J Microsc Ultrastruct 2015; 3:137–147. https://doi.org/10.1016/j.jmau.2015.03.001

21. Erdemli ME, Altinoz E, Aksungur Z, Turkoz Y, Dogan Z, Gozukara Bag H. Biochemical investigation of the toxic effects of acrylamide administration during pregnancy on the liver of mother and fetus and the protective role of vitamin E. J Matern Neonatal Med 2017; 30:844–848. https://doi.org/10.1080/14767058.2016.1188381

22. Hasanin NA, Sayed NM, Ghoneim FM, Al-Sherief SA. Histological and ultrastructure study of the testes of acrylamide exposed adult male albino rat and evaluation of the possible protective effect of vitamin E intake. J Microsc Ultrastruct 2018; 6:23. https://doi.org/10.4103/jmau.jmau_7_18

23. Oleshchuk O, Ivankiv Y, Falfushynska H, Mudra A, Lisnychuk N. Hepatoprotective effect of melatonin in toxic liver injury in rats. Medicina (B Aires) 2019; 55:304. doi: 10.3390/medicina55060304

24. Bicer Y, Elbe H, Karayakali M, Yigitturk G, Yilmaz U, Cengil O, Al Gburi MRA, Altinoz E. Neuroprotection by melatonin against acrylamide-induced brain damage in pinealectomized rats. J Chem Neuroanat 2022; 125:102143. https://doi.org/10.1016/j.jchemneu.2022.102143

25. Kopańska M, Batoryna M, Banaś-Ząbczyk A, Błajda J, Lis MW. The Effect of α-Tocopherol on the Reduction of Inflammatory Processes and the Negative Effect of Acrylamide. Molecules 2022; 27:965. doi: 10.3390/molecules27030965

26. Famurewa AC, Edeogu CO, Offor FI, Besong EE, Akunna GG, Maduagwuna EK. Downregulation of redox imbalance and iNOS/NF-κB/caspase-3 signalling with zinc supplementation prevents urotoxicity of cyclophosphamide-induced hemorrhagic cystitis in rats. Life Sci 2021; 266:118913. https://doi.org/10.1016/j.lfs.2020.118913

27. Hamid M, Liu D, Abdulrahim Y, Liu Y, Qian G, Khan A, Gan F, Huang K. Amelioration of CCl4-induced liver injury in rats by selenizing Astragalus polysaccharides: Role of proinflammatory cytokines, oxidative stress and hepatic stellate cells. Res Vet Sci 2017; 114:202–211. https://doi.org/10.1016/j.rvsc.2017.05.002

28. Erdemli ME, Zayman E, Erdemli Z, Gul M, Gul S, Gozukara Bag H. Protective effects of melatonin and vitamin E in acetamiprid-induced nephrotoxicity. Environ Sci Pollut Res 2020; 27:9202–9213. https://doi.org/10.1007/s11356-019-06754-y

الملخص العربى

الحماية الكبدية المحتملة التي يعززها كلا من الميلاتونين والألفا توكوفيرول في إصابة الكبد المستحثة بمادة الأكريلاميد في ذكور الجرذان البيضاء: دراسة نسيجية وكيميائية مناعية

هند رجب موسى¹، احمد عبد الرحمن مرسى²، لمياء محمد شوقى³

¹قسم التشريح ـ كليه الطب ـ جامعة بنها

²قسم الهستولوجيا ـ كلية الطب ـجامعة الفيوم

³قسم الهستولوجيا ـ كلية الطب ـجامعة بنها

المقدمة: توجد مادة الاكريلاميد فى البيئة المحيطة بشكل شائع لأنها تتكون فى الاطعمة التى تطهى تحت ظروف خاصة من الحرارة العالية. أكدت العديد من الدراسات السابقة سمية الاكريلاميد على أعضاء الجسم المختلفة.

الهدف: تهدف الدراسة الحالية إلى التحقق من مدى الكفاءة المحتملة لكلا من فيتامين هـ والملاتونين في حماية الكبد من السمية المستحثة بالاكريلاميد في ذكور الجرذان البيضاء. ايضا، تم فحص الآليات المفترضة المساهمة في هذه الحماية باستخدام الدراسات النسيجية والكيميائية النسيجية المناعيه.

المواد والطرق المستخدمة: تم تقسيم ٤٩ من ذكور الجرذان البيضاء الى سبع مجموعات متساوية. المجموعة الضابطة، مجموعة فيتامين هـ (١٠٠ مجم / كجم / يوم)، مجموعة الميلاتونين (١٠ مجم / كجم / يوم)، مجموعة الاكريلاميد (٥ مجم / كجم / يوم ، مجموعة الاكريلاميد/ فيتامين هـ ، مجموعة الاكريلاميد/ الميلاتونين، مجموعة الاكريلاميد/فيتامين هـ /الميلاتونين. تم إعطاء العلاج لجميع المجموعات يوميا عن طريق الفم لمدة ٨ أسابيع. في نهاية التجربة، تم سحب عينات الدم لقياس إنزيمات الكبد. تم استئصال الكبد وتجهيزه لقياس تركيزات العوامل المؤكسده ومضادات الاكسدة فى انسجة الكبد . كما تم تحضير عينات نسيجية بشمع البرافين وصبغها بالهيماتوكسلين والأيوسين. كما تم استخدام صبغة الماسون . تم إجراء فحوصات كيميائيه مناعيه للكشف عن التعبير المناعي لبروتينات الباكس، بى.سى.ال٢ و اى نوس.

النتائج: أظهرت الجرذان المعرضة للاكريلاميد تغيرا ملحوظًا في التحليلات البيوكيميائيه، بالإضافة إلى تغير اصطفاف خلايا الكبد والتغيرات التحلليه فى صورة فجوات خلوية والتي لوحظت في نتائج الهيماتوكسيلين والايوسين. كذلك لوحظ زيادة فى تراكم النسيج الليفى عند استخدام صبغة الماسون. واختلال ظهور البروتينات التى تم الكشف عنها بالصبغة الكيميائيه النسيجيه المناعيه. أدى العلاج بفيتامين هـ أوالميلاتونين إلى تحسين التغيرات النسيجية والكيميائية الحيوية مع استعادة التركيب الطبيعى عند استخدام العقارين معا .

الخلاصة: قام كلا من فيتامين هـ والميلاتونين بحماية الكبد من السمية الكبدية المستحثة بالاكريلاميد، وقد يتم ذلك عن طريق إعادة التوازن بين عوامل ومضات الأكسدة، تقليل ظهور البروتينات المؤيدة لموت الخلايا المبرمج، وزيادة ظهور البروتينات المضادة لموت الخلايا المبرمج، وتثبيط مسارات الالتهاب عند اعطاء الدوائين مجتمعين، كان هناك تاثير تازرى لكل منهما.